Cumhuriyet Sci. J., 46(4) (2025) 841-853
DOI: https://doi.org/10.17776/csj.1671518

Cumhuriyet Science Journal

| csj.cumhuriyet.edu.tr | Founded: 2002 ISSN: 2587-2680 e-ISSN: 2587-246X Publisher: Sivas Cumhuriyet University

Synthesis, Characterization of a Schiff Base Ligand and Its metal complexes, Their Catalytic, Thermal and DNA Binding Features

Selma Bal [1, a,*]

[1] *Kahramanmaraş Sütçü İmam Üniversitesi Fen Fakültesi, Kimya Bölümü, Avşar Kampüsü, 46100, Kahramanmaraş, Türkiye*

**Corresponding author*

Research Article

History
Received: 07/06/2025
Accepted: 29/11/2025

ABSTRACT

This work, first of all, reports the synthesis and structural elucidation of a schiff base ligand and its Co(II), Ni(II)and Mn(II) coordination compounds using various spectroscopic methods. Then, it moves on to the search of catalytic activity features of all the metal complexes, which were tested on the oxidation reactions of styrene and cyclohexene that are known to have a crucial importance in organic synthesis. The results of these reactions showed that the metal complexes especially the Cobalt complex was the most effective as catalyst, showing %70.3 yield for styrene oxidation and %50.1 yield for cyclohexene. Synthesized compounds were also searched for their thermal behaviour and similar fragmentations were observed only for the Cobalt and Manganese complexes of the ligand. Finally DNA binding studies were carried out on all the synthesized compounds and among them the Manganese complex showed the highest binding constant (K_b) with 7.04.

Keywords: Catalysis, Coordination, DNA binding, Schiff base,

[a] selmabal@ksu.edu.tr https://orcid.org/0000-0001-9547-8717

Introduction

Schiff bases, due to their easy synthesis and stability, have become one of the most important organic compounds [1-4]. In many biological systems such as pharmacy, medicine and chemical catalysts these imines and their coordination compounds showed great importance as antimicrobial, anticancer and antiviral [5-11]. In bioinorganic mechanisms, transition metals catalysing the transfer of oxygen atoms to organic substrates have been studied over the years. Especially the soluable transition metal complexes in alkene oxidations as catalysts have captured great attention [12-15]. Because many catalytic reactions are carried out in high temperatures it is important to use catalysts stable to higher temperatures and various schiff base complexes have been examined for their thermal behaviour throughout the years as well as for their various biological activities [16-19]. DNA, on the other hand, remains as an utterly important biological target for developing new drugs [20] and many factors, like the ligand type and the coordination geometry, influence the ability to engage with the DNA [21]. In light of these factors, some Schiff bases were being searched for their binding interactions with DNA [22-28]. Although the most known chemotherapeutic drugs belonged to cis-platinium family like cisplatin, carboplatin and oxaliplatin, due to their side effects and toxicity, it has become a major target to develop non-platinum based dugs for DNA binding studies.

Results and Discussion

Spectral Analysis

1H NMR spectra of our Schiff base ligand Scheme-1 gave a quartet (J= 7.2 Hz) at 4.38 ppm and a triplet (J= 7.2 Hz) at 1.47 ppm corresponding to the ethyl group attached to the nitrogen atom on the carbzole unit [14]. The sharp singlet recorded at 1.36 ppm belonged to the three methyls in the tert-butyl group on the phenolic ring. The imine proton (H-16) gave a singlet at 8.85 ppm [12,14].

All the aromatic protons gave signals in the reagion between 6.55 ppm and 8.65 ppm, mostly overlapped with each other. The three methyl protons on the phenolic ring, however, gave a sharp singlet at 1.36 ppm. The singlet seen at furthest downfield at 10.07 ppm belonged to the hydroxyl proton. 13C NMR spectra gave the imine carbon signal at 157.7 ppm. The signals of the ethyl group attached to nitrogen in the carbazole were seen at 13.9 ppm and at 37.8 ppm. The sharp long signal at 31.7 corresponded to the three methyl carbons on the tertiary group and the short signal at 34.5 belonged to the tertiary carbon itself. The other aromatic ring carbons gave carbon peaks between 107 and 160 ppm [14].

Examination of the IR spectra of the synthesized compounds revealed weak signals at 1610 and 1669 for the imine (C=N) stretchings. This stretching was red shifted in the complexes. Aromatic C-H stretchings were at 2990 and 3000 cm-1. The broad signals at around 3400 cm-1 belonged to O-H stretchings in the phenolic group. C-N stretchings were at 1195 cm-1. Symmetric and asymmetric stretchings of aliphatic C-H on the other hand, were between2922 cm-1 and 2972 cm-1. The three intense bands seen in the IR spectra of the coordination compounds corresponded to the carboxylate stretchings of the acetates. These stretchings are categorized as asymmetric and symmetric, proving the chelations between carboxyl groups with metals. The difference between these asymmetric and symmetric stretchings tells us about the modes of the coordiations (e.g. bridging, bidentate or unidentate) [29,30]. And the examination of the differences between these asymmetric and symmetric stretchings gave values of higher than 200 cm-1,which proves the unidentate carboxylate chelations of the acetates present in the coordination compounds [29,30] The results of these calculations can be seen in Table 1 below.

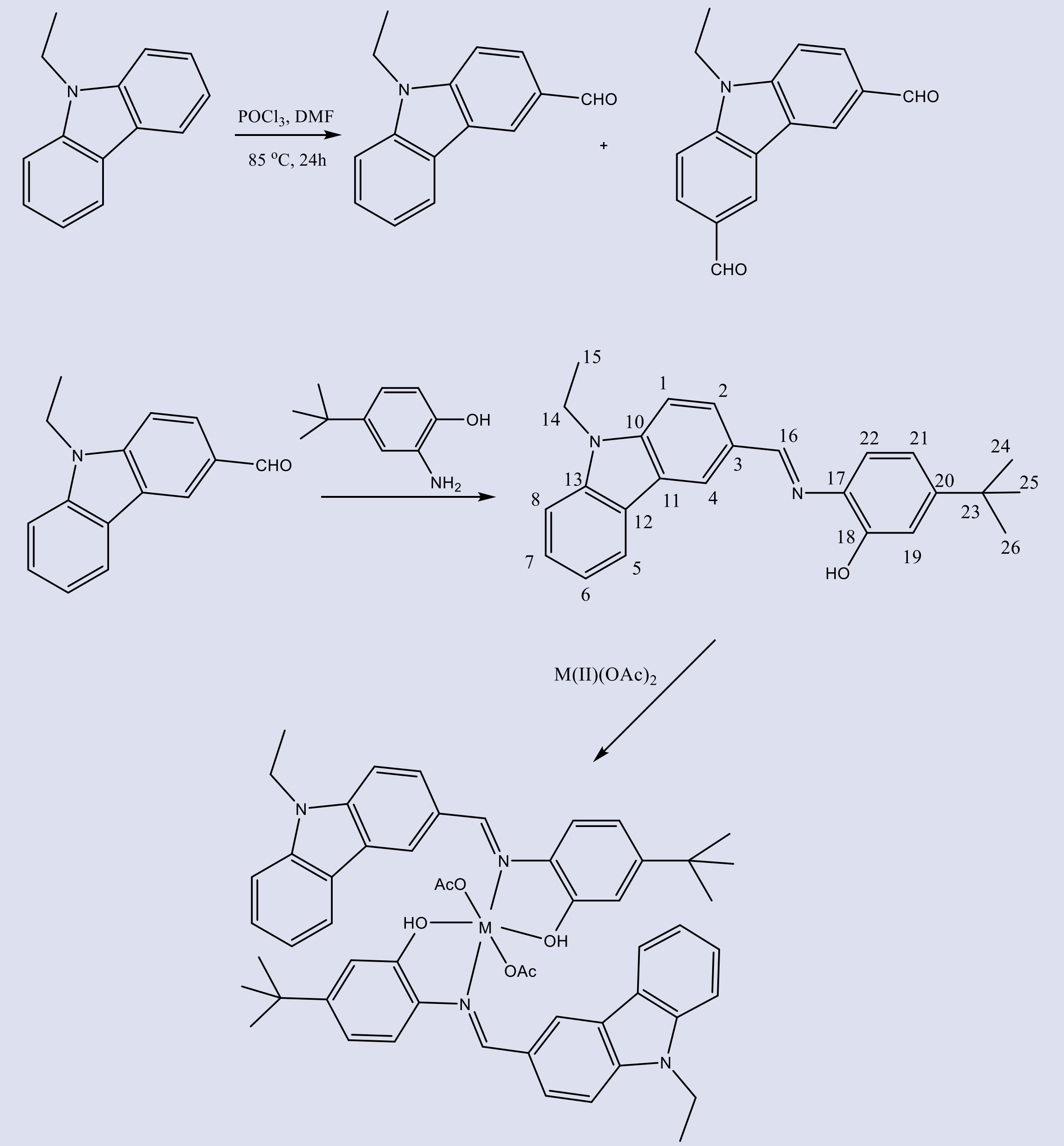

Scheme-1. Synthesis scheme of the ligand and the coodination compounds.

Table 1. Asymmetric and symmetric IR values of carboxylate coordinations and the difference between them

Complex	$\nu_{asymmetric}$	$\nu_{symmetric}$	Δ ($\nu_{asymmetric}$-$\nu_{symmetric}$)
$Mn(L)_2(OAc)_2$	1685,1580	1230	455, 350
$Co(L)_2(OAc)_2$	1689,1582	1233	456, 349
$Ni(L)_2(OAc)_2$	1687,1583	1235	452, 348

In the EDAX (energy dispersive X-ray analysis) spectra, characteristic Kα and L� values were obtained for the synthesized complexes. Examination of scanning electron microscopy, which is SEM in short, gave ideas about the surface morphology of the coordination compounds. The images of EDAX proved the existance and the purity of metals and all the SEM photographs gave homogeneous matrixes of the coordination compounds. Figures 1-4 can be examined for the Ligand and complexes Ni(L)2(OAc)2, Co(L)2(OAc)2, and Mn(L)2(OAc)2. To detect the presence of the metals, the EDXRF (energy dispersive X-ray fluorescence) experiments were carried out on the complexes. By this technique, chemical elements, subjected to appropriate excitation, emit characteristic radiations [31]. In other words, the inner shell vacancies of the atoms are filled by electron transitions from outer orbitals by excitation, which leads to characteristic X-ray emissions [32]. These characteristic X-rays were measured by high-resolution Si(Li) detector, and the area under the K� peaks of Cobalt. Manganese and Nickel were used to calculate the concentration values. The results were given in Table 2, which were in consistent with the calulated values.

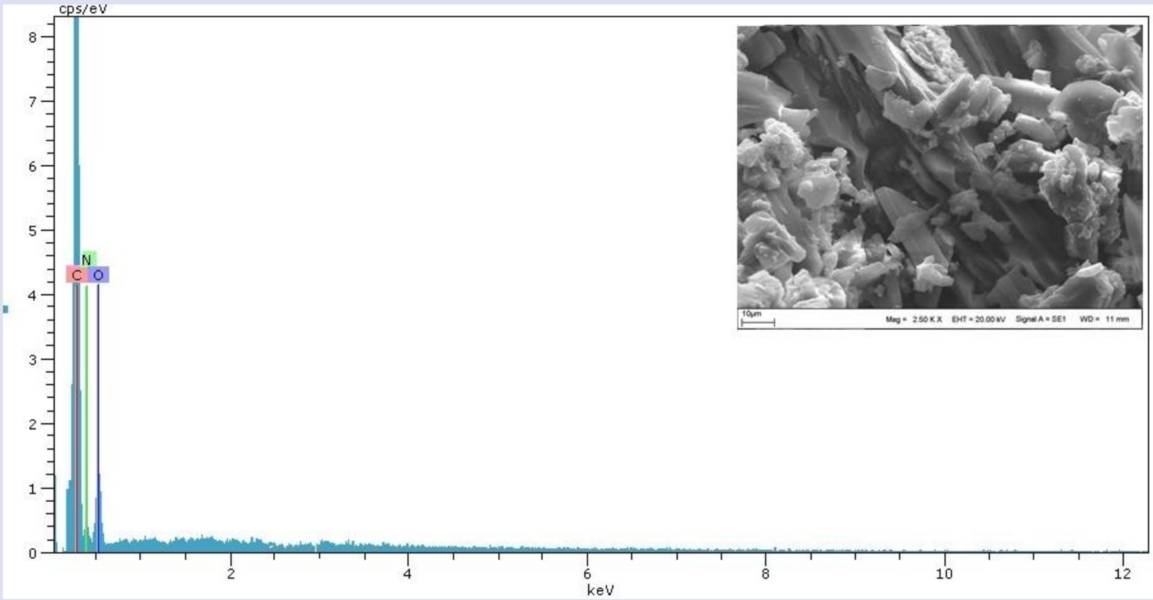

Figure-1. EDAX spectrum of L and its SEM photograph.

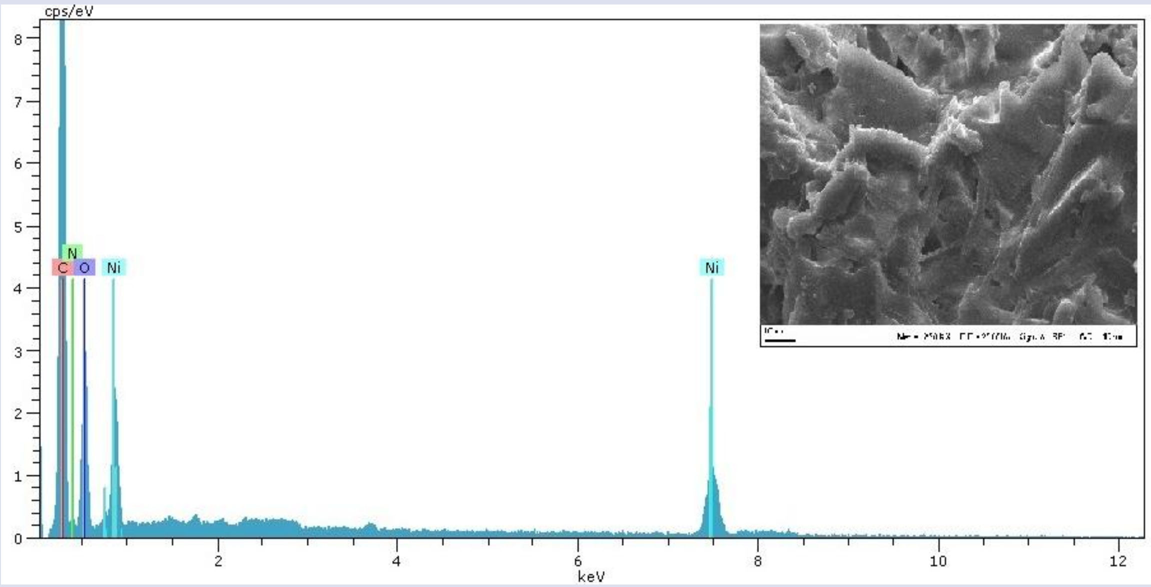

Figure-2. EDAX spectrum of complex $Ni(L)_2(OAc)_2$ and its SEM photograph.

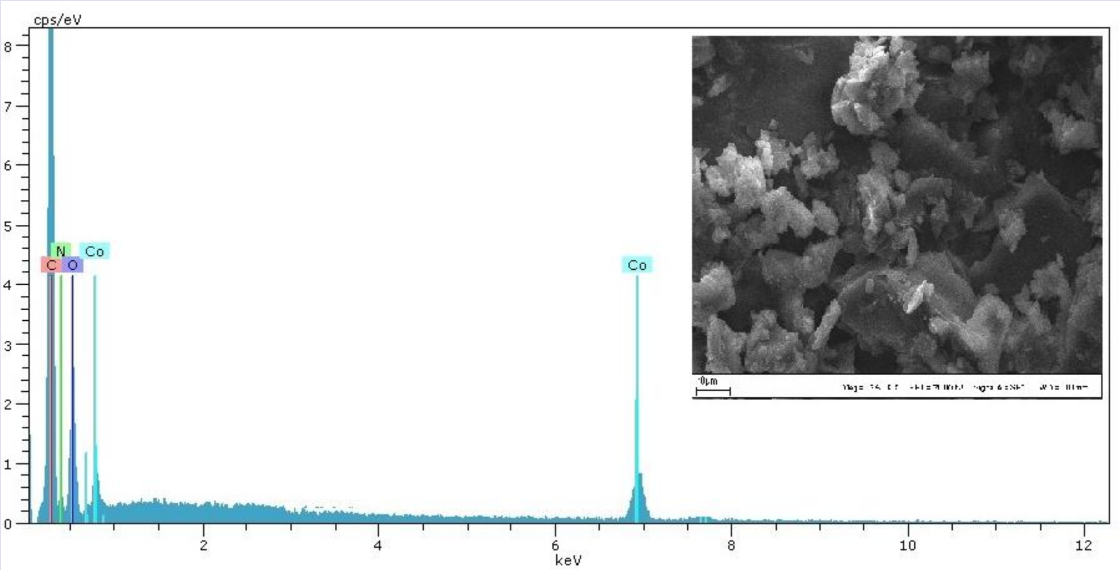

Figure-3. EDAX spectrum of complex $Co(L)_2(OAc)_2$ and its SEM photograph.

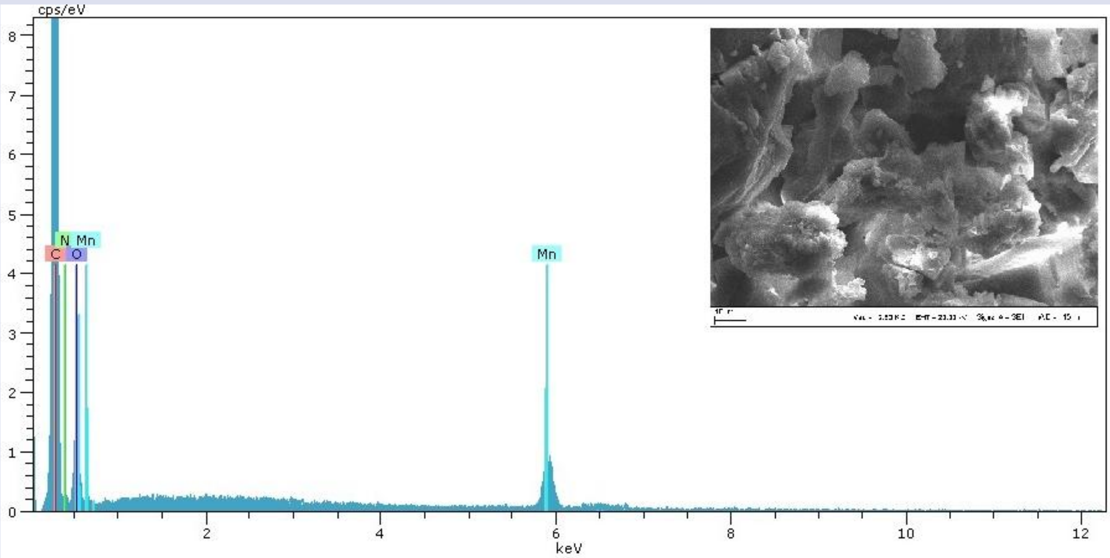

Figure-4. EDAX spectrum of complex Mn(L)2(OAc)2 and its SEM photograph.

Table 2. Estimated metal percentages by EDXRF

Complex	Chemical Formula	Calculated Value/%	Experimental Values (EDXRF)/%
$Mn(L)_2(OAc)_2$	$C_{54}H_{58}MnN_4O_6$	6.02	6±0.3
$Co(L)_2(OAc)_2$	$C_{54}H_{58}CoN_4O_6$	6.43	6±0.3
$Ni(L)_2(OAc)_2$	$C_{54}H_{58}NiN_4O_6$	6.40	6±0.3

The LCMS spectra of all the synthesized compounds gave parent ion peaks of [M]+ or [M++1]. In addition we were able to see the ligand mass peaks in all the mass spectra of the complexes. The geometries of all the coordination compounds were concluded from the magnetic susceptibility studies to be octahedral. For example, 5.06, 6.10 and 4.5 B.M. magnetic moments were calculated for Cobalt, Manganese and Nickel coordination compounds respectively [33-35]

Catalytic Activity

Oxidation and epoxidation reactions are extremely important for organic chemistry and they are used either as starting compounds or as transition reactions. Therefore, the catalytic activity features of the synthesized complexes were exmined in the oxidation reactions of cyclohexene and styrene (Scheme 2). All the reactions have been carried out in acetonitrile at 80 oC. In these experiments styrene oxidation reactions gave better results than the cyclohexene. Among all of the oxidation reactions only the Manganese complex gave the lowest yields. For example, Co(II) and Ni(II) complexes gave %70.3 and %62.2 percentages while the manganese complex gave %53.4 styrene convertion. Cyclohexene conversions were the lowest in these experiments. All the catalytic activity results can be seen in Table 3 and Table 4.

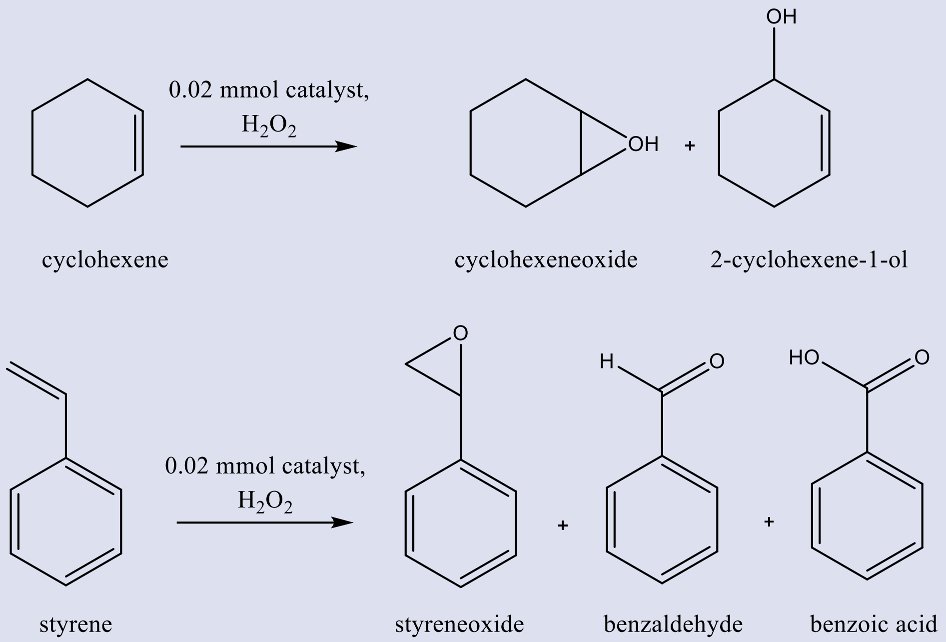

Scheme-2. Oxidation schemes of cyclohexene and styrene.

Table 3. Catalytic activity results on Styrene

		Selectivity (%)		
Catalyst	**Styrene conversion (%)**	**Styrene oxide**	**Benzaldehyde**	**Benzoic acid**
$Mn(L)_2(OAc)_2$	53.4	40.7	39.3	6.4
$Co(L)_2(OAc)_2$	70.3	56.5	51.7	8.3
$Ni(L)_2(OAc)_2$	62.2	52.6	48.4	5.8

Table 4. Catalytic activity results on cyclohexene

		Selectivity (%)	
Catalyst	**Cyclohexene conversion (%)**	**Cyclohexene oxide**	**2-Cyclohexene-1-ol**
$Mn(L)_2(OAc)_2$	31.7	13.9	10.8
$Co(L)_2(OAc)_2$	50.1	29.3	15.5
$Ni(L)_2(OAc)_2$	41.3	25.6	14.6

Thermogravimetric Analysis

Thermal spectra of the synthesized compounds revealed similar degradation steps starting at around 200 oC. The ligand itself gave two mass losses with 52,43%, which was calculated as the carbazole unit (C14H12N) and 47,56 % corresponding to the phenolic group (C11H14NO) with the imine (-CH=N-). Among the coordination compounds Cobalt and Manganese gave almost identical mass losses. For example, between 200 oC and 300 oC loss of phenolic group with the imine occurred with 38,38 % and 38,55 % for Cobalt and Manganese complexes respectively. Following this, a small mass loss of 12,86 % (for Cobalt complex) and 12,92 % (for Manganese complex) were recorded. And finally the biggest loss occurred between 425-800 oC corresponding to the two carbazole units in Cobalt and Manganese coordination compounds with 42,31 % and 42,49 % respectively. However, the Nickel complex revealed only two degradation steps. First step showed a mass loss of 76,79 % corresponding to two phenolic groups without the hydroxyls and two carbazole units with the imine group. The second step, revealed a total mass losses of the two acetyls, two hydroxyls and the Nickel itself. All the thermal graphics and the results can be seen in Figure 5 and Table 5.

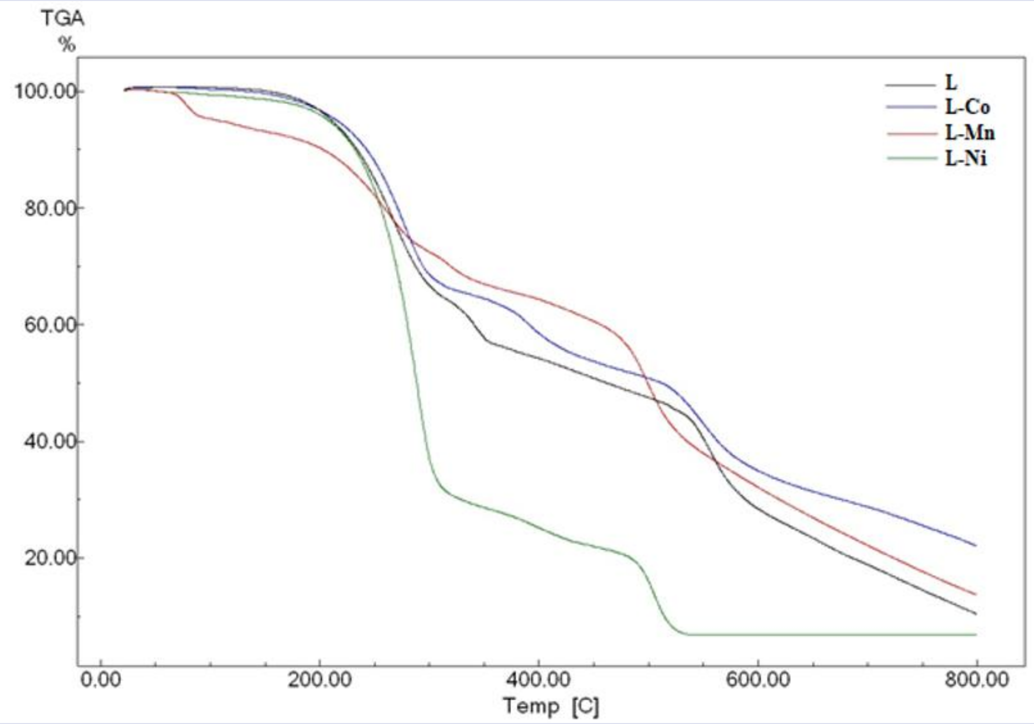

Figure 5. Thermal graphics of the synthesized compounds

Table 5. Thermal analysis of the synthesized compounds

Compounds	Formula	Mass	Temperature °C	Mass Loss %	Fragments
L	$C_{25}H_{26}N_2O$	370	200-400 350-600	52,43 47,56	$C_{14}H_{12}N$ $C_{11}H_{14}NO$
$Co(L)_2(OAc)_2$	$C_{54}H_{58}CoN_4O_6$	917	200-300 300-380 380-800	38,38 12.86 42,31 6,45	$2(C_{11}H_{14}NO)$ $2(OCOCH_3)$ $2(C_{14}H_{12}N)$ Co
$Mn(L)_2(OAc)_2$	$C_{54}H_{58}MnN_4O_6$	913	200-300 300-380 380-800	38.55 12.92 42.49 6,04	$2(C_{11}H_{14}NO)$ $2(OCOCH_3)$ $2(C_{14}H_{12}N)$ Mn
$Ni(L)_2(OAc)_2$	$C_{54}H_{58}NiN_4O_6$	916.7	200-350 350-600	76,79 22,97	$2(C_{10}H_{12})$ $2(C_{15}H_{13}N_2)$ $2(CH_3COO)$ $2(OH)$ Ni

DNA Binding Studies

DNA binding

DNA binding studies by UV-vis absorption titration were performed for compounds with fixed compound concentrations (10 µM). Therefore, they were dissolved in DMSO to obtain a stock solution of the compounds. The titration of the compounds was carried out using a fixed concentration of different DNA concentrations. λmax was noted. DNA binding coefficients (Kb) were solved by the Benassi-Hildebrand equation (Eq. 1) as by [36]. Equivalent is as follows:

$$\text{In } [DNA]/(\varepsilon a-\varepsilon f) = [DNA]/(\varepsilon b-\varepsilon f) + 1/Kb(\varepsilon b-\varepsilon f) \quad (1)$$

the equation given above, [DNA] is the DNA concentration in base pairs. A, ⍰f and ⍰b corresponds to the molar absorption coefficients of aggregated / [ligand], free ligand and ligand-DNA solutions. Kb indicates the strength of the ligand to bind to DNA and is calculated from the slope of the line drawn between [DNA] / (εa – εf) and [DNA].

Relocation studies with EB

It has been previously explained that while an increase in EB fluorescence emission is observed when DNA is intercalated between base pairs, replacement of EB by another molecule causes the emission of EB to be quenched, indicating that the new molecule binds to DNA by intercalation or by binding to grooves [37]. To 50 µM FS-DNA solutions pretreated with 5 µM EB in Tris-HCl, compounds (in different concentrations) were added. Emission spectra were then recorded at excited at λex = 526 nm in the 500-750 nm wavelength range. The quenching constants (QC) were determined by means of the Stern-Volmer equation.

$$I_0/I = 1 + K_{sv}[Q] \quad (2)$$

I0 and I are the fluorescence intensities in absence and presence of complexes. [Q] is total quenching concentration.

$$Log(I_0–I)/I = log\ K_F + n\ log[Q] \quad (3)$$

Plotting *log* (I_0-I) versus *log* [Q] and determining the number of binding sites per base (n) from the slope of the resulting line.

UV–vis absorbance titrations

Electronic absorption spectroscopy is an effective method to study the binding modes of metal complexes with DNA. The red shift and hypochromism occurring during measurements are related to the binding of metal complexes to DNA due to the intercalative mode involving a strong stacking interaction between the aromatic chromophore of the complexes and the base pairs of DNA [38]. Hyperchromism, on the other hand, indicated that the compounds and metal complexes exhibited groove binding with DNA [39]. The absorption spectra of the ligand and metal complexes in the absence and presence of FSds-DNA are shown in Figs 6-9. As presented in (Fig.9) and (Fig. 10), when titrated with FSds-DNA, a hyperchromism of 45% was observed in the absorption band of the ligand L and a blue shift in wavelength of 1.3 nm was observed. This indicated that the ligand can bind with DNA via groove binding. When we examined the interaction of the metal complexes, we observed an increase in the absorption bands with the addition of DNA and a blue shift of approximately 2-3 nm in the wavelengths. These spectral features suggest that both the ligand and the complex interact with FSds-DNA via a minor grove mode, most likely involving π-π stacking interactions between the base pairs of DNA. The binding constants of the compounds are given in Table-6. The highest binding value among the compounds is L-Mn (Kb=7.04 x104), which has a tert-butyl Mn complex in its structure. The DNA binding values of the metal complexes can be given as L-Mn>L-Ni>L-Co, respectively. The tert-butyl group in the structure is thought to originate from the Vander Wals interaction with DNA.

Fluorescence studies were conducted to fully understand the DNA binding mode of the compounds.

Table 6. The binding constant (K_b), quenching constant (*K*sv) and number of binding sites (n) for the interactions of the compounds with EB DNA

Compounds	$K_b\ 10^4$	$K_{sv}\ 10^4$	$logK_b$	Kb 10^4	n
L	3.5	1	4.99	9.7	1.27
L-Mn	7.04	9.4	3.02	1.04	0.76
L-Co	5.15	3.2	3.03	1.07	0.669
L-Ni	6.48	2.6	2.09	0.123	0.699

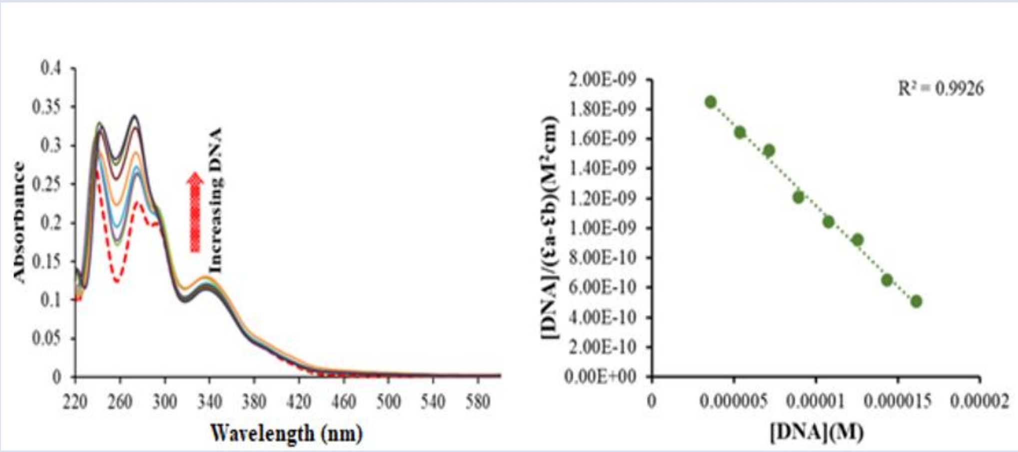

Figure 6. The electronic absorption spectra of the L-Ni (15µM) -DNA complex in the presence of increasing amounts of FSds-DNA (0-110 µM). The plots of [DNA]/(εa – εf) versus [DNA] for the compounds with FSds-DNA.

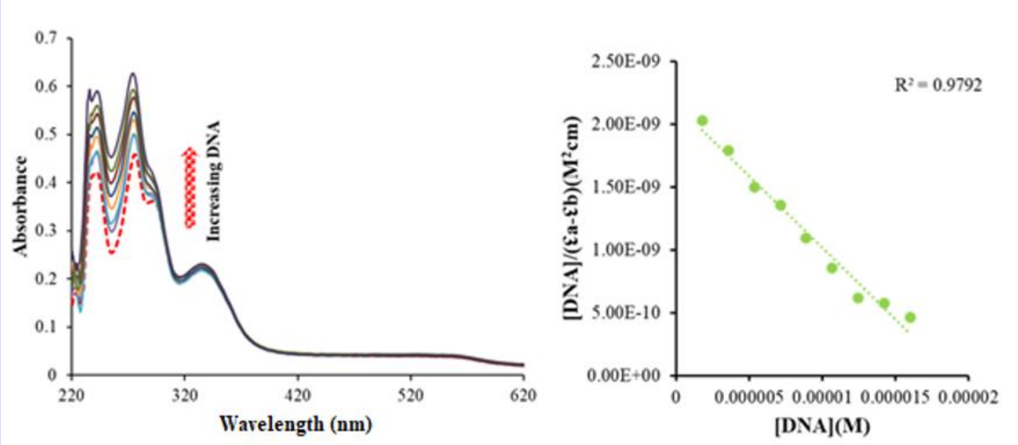

Figure 7. The electronic absorption spectra of the L-Co (55µM) -DNA complex in the presence of increasing amounts of FSds-DNA (0-100 µM). The plots of [DNA]/(εa – εf) versus [DNA] for the compounds with FSds-DNA.

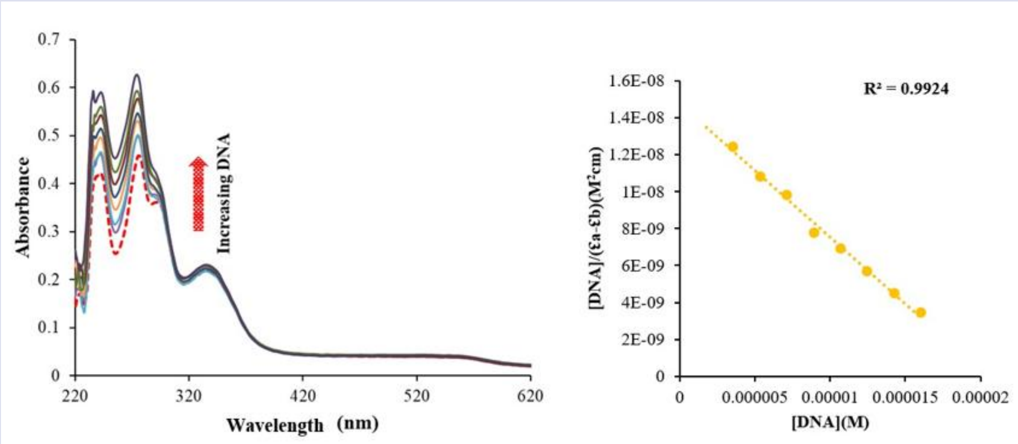

Figure 8. The electronic absorption spectra of the L-Mn (45µM) -DNA complex in the presence of increasing amounts of FSds-DNA (0-90 µM). The plots of [DNA]/(εa – εf) versus [DNA] for the compounds with FSds-DNA.

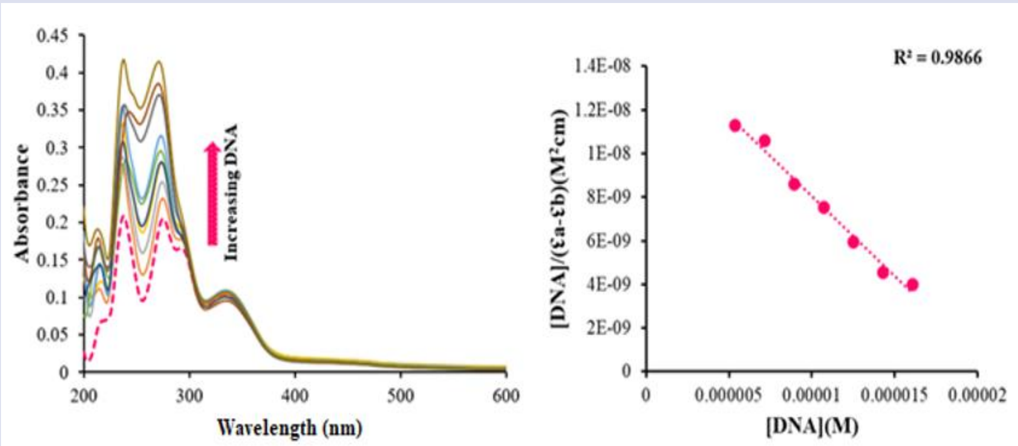

Figure 9. The electronic absorption spectra of the ligand L (25µM) -DNA complex in the presence of increasing amounts of FSds-DNA (0-90 µM). The plots of [DNA]/(εa – εf) versus [DNA] for the compounds with FSds-DNA.

Fluorescence study

Ethidium bromide (EB) is a well known fluorophore that is widely used to study the binding mode of the interaction between drugs and DNA. Due to the robust linkage between DNA base pairs, the fluorescence intensity of EB is enhanced in the presence of FSdsDNA. The addition of a second molecule has previously been reported to quench the increased emission intensity [40]. DNA by the same binding mode, displacing EB from the DNA helix, thereby reducing the fluorescent intensity of the EB-DNA system [41] . EB is a known probe that similarly associates with DNA [42] . The emission spectra of EB bound to FSdsDNA and the continuous addition of ligands and complexes to these systems are shown in

Figures 10-13. With the addition of the compounds, the ligand and metal complexes showed a decrease in the fluorescence intensity of EB-DNA by 55%, 70%, 53% and 51%, respectively. This suggests that the compounds do not displace EB from the base pair of FSdsDNA helices. Therefore, it is clear from this result that the compounds do not bind to FSdsDNA in a non-intercalative mode. It is also known that a decrease in emission intensity occurs when the compounds bind to another region of the DNA chain or when they are replaced by water molecules. The Ksv values of EB dye bound to FSdsDNA by ligand and metal complexes were calculated from (equation 2) using the Stern-Volmer plot [43] as shown in Figures 10-13.

$$I_0/I = 1 + K_{sv}[Q] \quad (2)$$

It was determined that the compound with the highest Ksv value was the L-Mn complex containing Mn in its structure (Ksv= 9.4 x10^4 M). Manganese binding abilities were previously searched by Luck & Zimmer. And they found that Mn2+ was stabilizing the secondary structure of DNA through electrostatic interactions with the negatively charged phosphate regions. It has been determined that Mn2+ can destabilize the secondary structure of DNA under low ionic conditions [44]. The n and log Kb values indicate the binding site with DNA. As can be seen from the n values given in Table 6, the ligands and complexes bind to a single region of DNA [45]. The binding constant of the compound to DNA is also given in Table-6.

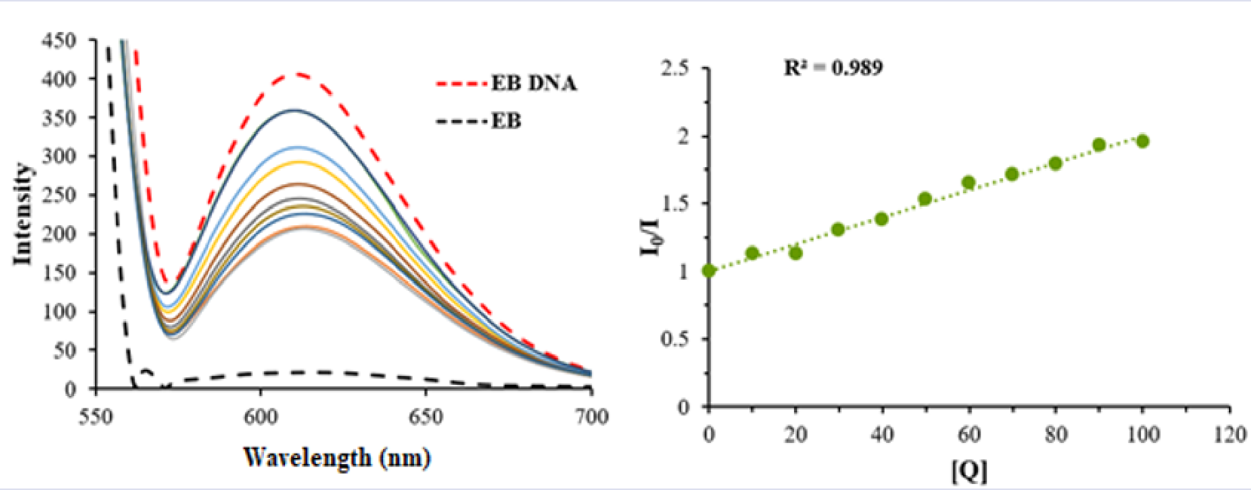

Figure 10. Fluorescence quenching curves of ethidium bromide bound to DNA: L. [DNA] = 50 µM, [EB] = 5 µM, and [L] = 0–110 µM The Stern–Volmer plots of the fluorescence titrations for the L.

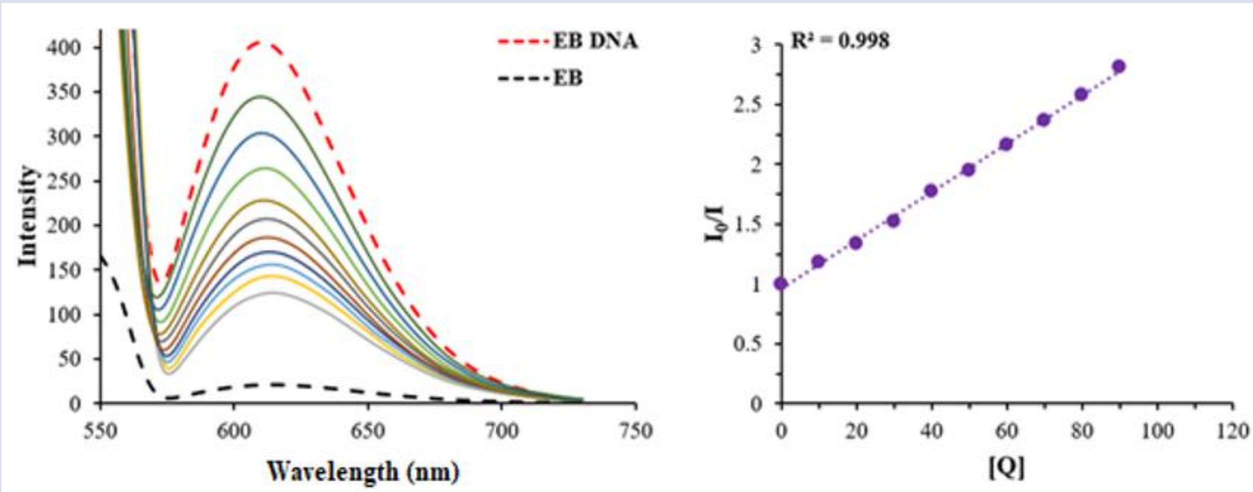

Figure 11. Fluorescence quenching curves of ethidium bromide bound to DNA: L-Co. [DNA] = 50 µM, [EB] = 5 µM, and [L-Co] = 0–130 µM The Stern–Volmer plots of the fluorescence titrations for the L-Co.

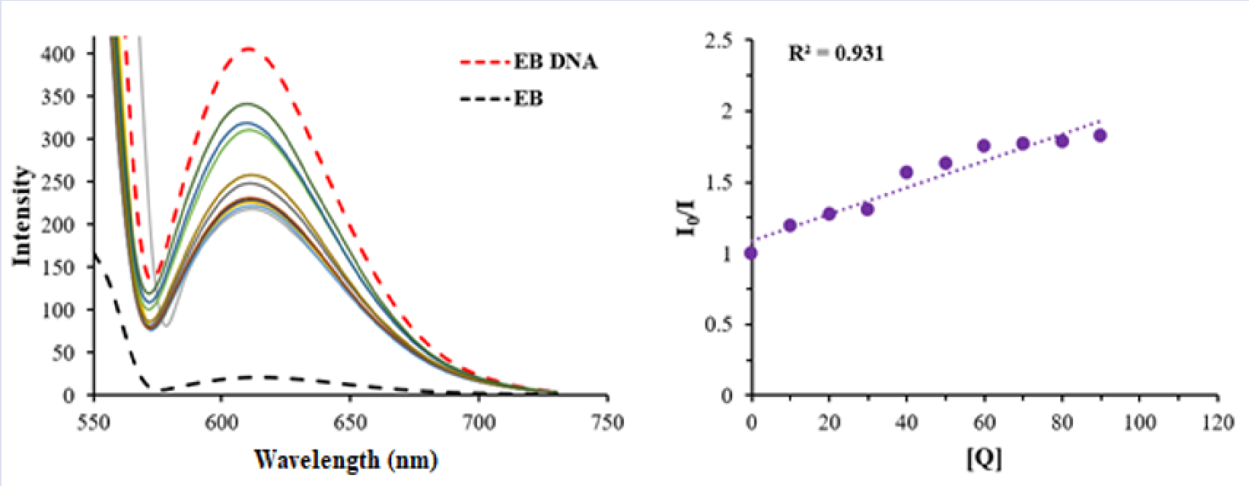

Figure 12. Fluorescence quenching curves of ethidium bromide bound to DNA: L-Mn. [DNA] = 50 µM, [EB] = 5 µM, and [L-Mn] = 0–80 µM The Stern–Volmer plots of the fluorescence titrations for the L-Mn.

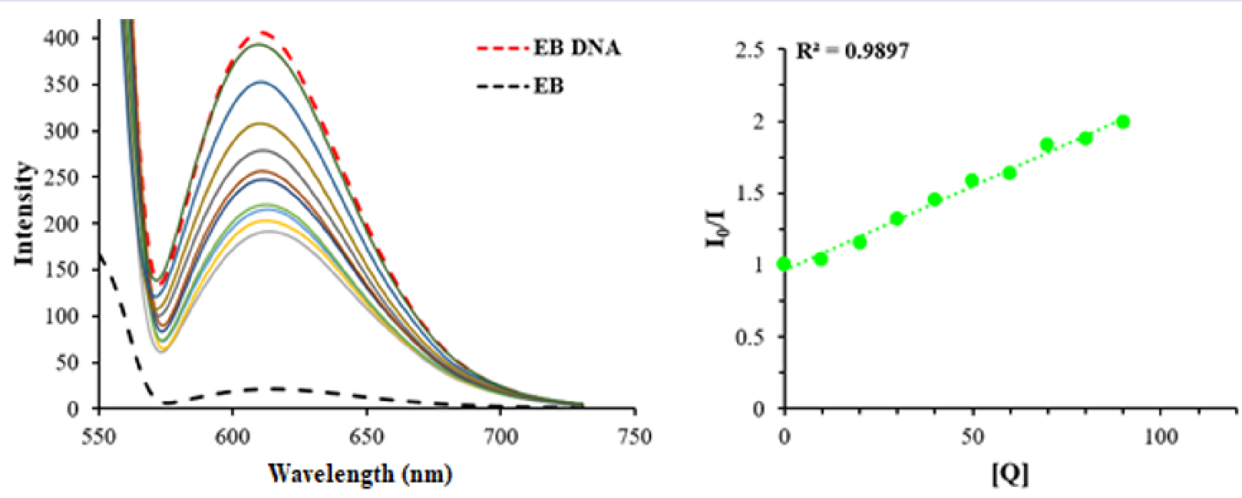

Figure 13. Fluorescence quenching curves of ethidium bromide bound to DNA: L-Ni. [DNA] = 50 µM, [EB] = 5 µM, and [L-Ni] = 0–120 µM The Stern–Volmer plots of the fluorescence titrations for the L-Ni.

Experimental

The acetate salts of the transition metals Copper, Cobalt and Nickel, 2-amino-4-ethylphenol, phosphorus(V) oxychloride and 9-ethylcarbazole were all purchased from sigma aldrich. Proton and carbon nmr spectra were taken on Bruker AV 400 MHz spectrometer in the solvent deuterated chloroform (CDCl3). Infrared spectra were taken in the region of 400-4000 cm-1on Schimadzu 8300 FT-IR spectrophotometer. U.V. spectra were taken on Schimadzu UV-160 A spectrophotometer in dimethyl sulfoxide with a concentration of 5.10^{-5} M for each compound. Mass spectra were obtained on LC/MS APCI AGILENT 1100 MSD spectrophotometer. The results of catalytic activity were analysed (examined) with the Schimadzu, GC-14B gas chromatograph equipped a flame ionization detector and a SAB-5 capillary. LECO CHNS 932 elemental analyzer was used for elemental analyses of all the synthesised compounds and the metal analyses were carried (performed) on an Ati Unicam 929 Model AA Spectrometer in solutions prepared by decomposing the compounds in aqua regia and subsequently digesting them in concentrated hydrochloric acid. Chemical compositions of all the compounds was obtained by EDAX, which was performed with Rönteck xflash detector analyzer was associated with a scanning electron microscope (SEM, Leo-Evo 40xVP). The energy spectra of the characteristic X-rays of the complex compounds were measured with Bruker energy dispersive X-ray spectroscope (EDX) by high-resolution Si(Li) detector. Incident electron beam energies from 3 to 30 keV had been used. In every case, the beam was at normal incidence to the sample surface and the measurement time was 100s. ZAF correction was used for all the EDAX spectra. ZAF correction takes atomic number (Z) absorption (A) and fluorescence excitation (F) effects into account when performing quantitative analysis. (Further), EDXRF (Energy dispersive X-ray fluorescence) was used for the detection of metals in the complexes and all the percentages were estimated using CATXRF program. Thermal analyses were performed on a PerkinElmer Thermogravimetric Analyzer TG/DTA 6300 instrument in the temperture range 30-800 °C with the heating rate of 10 °C/min under nitrogen atmosphere. Finally, Gouy method was used for the magnetic measurements. For this method, Hg[Co(SCN)4] was used as calibrant. The molar conductances of all the synthesized compounds were recorded using Jenway Model 4070 conductivity meter in MeOH (ca. 10^{-3}M).

Synthesis of the ligand and the complexes

Using POCl3 and Dimethylformamide, through Vilsmeyer reaction the N-ethylcarbazole was formylated. The resulted monoaldehyde and the dialdehyde were separated through flash chromatography using aceate and hexane mixture with the ratio of 1:10 as as outlined in literature [46,47]. The monoaldehyde (N-Ethylcarbazole-3-carbaldehyde) (1 mmol) was then reacted with 1 mmol 2-amino-4-tert-butylphenol (with the ratio of 1:1) in ethanol under reflux for 12 hours. This reaction resulted in 4-(tert-butyl)-2-(((9-ethyl-9H-carbazol-3-yl)methylene)amino)phenol as our ligand. This ligand, was then reacted with the acetate salts of the all related transition metals in ethanol and refluxed for 24 hours. The formed precipitates were recrystallised from methanol/ethanol (1:1) mixture.

L

4-(tert-butyl)-2-(((9-ethyl-9H-carbazol-3-yl)methylene)amino)phenol (C25H26N2O):

Yield 3.8 g (82 %); m.p.: 207 °C; ^{1}H NMR (400 MHz, $CDCl_3$): δ = 10.07 (s, OH), 8.85 (s, H-16), δ 8.65-δ 6.55 (Aromatic protons overlapped), 1.45 (t, *J* = 7.2 Hz, 3H-15), 4.39 (q, *J* = 7.2 Hz, 2H-14), 1.46 (t, *J* = 7.2 Hz, 3H-15), 1.36 (s, 3H-24, 3H-25, 3H-26), 13C NMR (100 MHz, $CDCl_3$): δ = 157.7 (C-16), , 37.8 (C-14), 13.9 (C-15), 31.7 (C-24, C-25, C-26), 34.5 (C-23). The rest of the carbon peaks were seen in the range δ 107 and δ 160. FT-IR(KBr): ν = 3150 (OH), 3050 (Aromatic C–H), 2985, 2935 (C–H), 1638 (CH=N), 1590 (Aromatic C=C), 1335, 1267 (OH bending) cm^{-1}; UV–Vis (DMSO, λmax, 1.0×10^{-5} M) = 240 (π-π*), 280(π-π*), 295(π-π*), 348(n-π*), 405(n-π*) nm; MS: m/z = 371.0 (M^++1); Λ_M = 1.9 Ω^{-1} cm^2 mol^{-1}.

$(L)_2Co(OAc)_2$

Di[2-[[(9-ethyl-9H-carbazol-3-yl)methylene]amino]-4-tert-butylphenol]cobalt(II) acetate

($C_{54}H_{58}CoN_4O_6$): Yield 1.7 g (74 %); m.p.: 227 °C; IR (KBr): ν = 3125 (OH), 3045 (Aromatic C–H), 2970, 2925 (C–H), 1620 (CH=N), 1578 (Aromatic C=C), 1680, 1585 (ν_{as}, COO^-), 1235 (ν_s, COO^-), 617 (ν_{as}, M–O), 597 (ν_s, M–O), 542 (M–N) cm^{-1}; UV–Vis (DMSO, λmax, 1.0×10^{-5} M) = 238 (π-π*), 276(π-π*), 285(π-π*), 351(n-π*) nm; MS: m/z = 917.2 (M^+); Λ_M = 23.1 Ω^{-1} cm^2 mol^{-1}.; μeff = 4.95 B.M.

$(L)_2Ni(OAc)_2$

Di[2-[[(9-ethyl-9H-carbazol-3-yl)methylene]amino]-4-tert-butylphenol]nickel(II) acetate

($C_{54}H_{58}N_4NiO_6$)Yield 1.38 g (63 %); m.p.: 227 °C; IR (KBr): ν= 3124 (OH), 3046 (Aromatic C–H), 2971, 2920 (C–H), 1617 (CH=N), 1580 (Aromatic C=C), 1681, 1586 (ν_{as}, COO^-), 1230 (ν_s, COO^-), 615 (ν_{as}, M–O), 589 (ν_s, M–O), 541 (M–N) cm^{-1}; UV–Vis (DMSO, λmax, 1.0×10^{-5} M) = 239 (π-π*), 274(π-π*), 295(π-π*), 345(n-π*), 400(n-π*) nm; MS: m/z = 918.0 (M^++1); Λ_M = 17.7 Ω^{-1} cm^2 mol^{-1}; μeff = 4.15 B.M.

$(L)_2Mn(OAc)_2$

Di[2-[[(9-ethyl-9H-carbazol-3-yl)methylene]amino]- 4-tert-butylphenol]manganese(II) acetate

($C_{54}H_{58}N_4NiO_6$)Yield 1.66 g (64 %); m.p.: 223 °C; IR (KBr): ν = 3110 (OH), 3050 (Aromatic C–H), 2978, 2932 (C–H), 1617 (CH=N), 1589 (Aromatic C=C), 1680, 1585 (ν_{as}, COO^-), 1240 (ν_s, COO^-), 617 (ν_{as}, M–O), 590 (ν_s, M–O), 541 (M–N) cm^{-1}; UV–Vis (DMSO, λmax, 1.0×10^{-5} M) = 235 (π-π*), 274(π-π*), 290(π-π*), 350(n-π*) nm; MS: m/z = 913.0 (M^+); Λ_M = 19.8 Ω^{-1} cm^2 mol^{-1}; μeff = 5.95 B.M.

Catalytic Activity Procedure

For the catalytic activity experiments, 1.10^{-3} mol catalyst, 20 ml acetonitrile (CH_3CN) as solvent, and 10 mmol cyclohexene or styrene were all stirred under nitrogen atmosphere for 8 h at 80 °C in a round-bottomed flask. The resulted mixture was then filtrated and washed with solvent and subjected to GC analysis.

Conclusion

With this work a schiff base ligand and its Co(II), Ni(II), Mn(II) complexes were synthesized, characterized and examined for their catalytic activiy, thermal behaviour, and for their DNA binding features. Catalytic activity results of all the coordination compounds showed good results on the oxidation reactions of cyclohexene and styrene. Examination of the thermal behaviors of all the synthesized compounds are quite important due to their usage in reactions requiring high temperatures and all the results were given in the results and discussion section. Finally the DNA binding studies of all the ompounds were examined thoroughly and they are found to make non-covalent bonding with the DNA. Especially the Manganese coordination compound was the most effective among other synthesized complexes.

Acknowledgement

I would like to thank Dr. Özge Güngör for interpreting the DNA binding studies.

Conflicts of Interest

There are no conflicts of interest in this work.

References

[1] Jeevadason A. W., Murugavel K. K., Neelakantan M. A., Review, types of piperazine-based Schiff base ligands: Synthesis, X-ray structures, magnetic studies and theoretical validation, *Inorganica Chimica Acta*, 503 (2020) 119439.

[2] Wang J., Zhang X., Liu H. B., Zhang D., Nong H., Wu P., Chen P., Li D., Aggregation induced emission active fluorescent sensor for the sensitive detection of Hg2+ based on organic–inorganic hybrid mesoporous material, *Spectrochimica Acta Part A: Molecular and Biomolecular Spectroscopy*, 227 (2020) 117585.

[3] Abu-Dief A. M., Mohamed I. M. A., A review on versatile applications of transition metal complexes incorporating Schiff bases, *Beni-Suef Univ. J. Basic Appl. Sci.*, 4 (2015) 119–133.

[4] Rollié S., Mangold M., Sundmacher K., Designing biological systems: systems engineering meets synthetic biology, *Chem. Eng. Sci.*, 69 (2012) 1–29.

[5] Liu X., Hamon J. R., Recent developments in penta-, hexa- and heptadentate Schiff base ligands and their metal complexes, *Coord. Chem. Rev.*, 389 (2019) 94–118.

[6] Marchetti F., Pettinari C., Di Nicola C., Tombesi A., Pettinari R., Coordination chemistry of pyrazolone-based ligands and applications of their metal complexes, *Coordination Chemistry Reviews*, 401 (2019) 213069.

[7] Marchetti F., Pettinari R., Pettinari C., Recent advances in acylpyrazolone metal complexes and their potential applications, *Coordination Chemistry Reviews*, 303 (2015) 1–31.

[8] Pahontu E., Julea F., Rosu T., Purcarea V., Chumakov Y., Petrenco P., Gulea A., Antibacterial, antifungal and in vitro antileukaemia activity of metal complexes with thiosemicarbazones, *Journal of Cellular and Molecular Medicine*, 19(4) (2015) 865–878.

[9] Tajudeen S. S., Kannappan G., Schiff base – copper (II) complexes: Synthesis, spectral studies and anti-tubercular and antimicrobial activity, *Indian Journal of Advances in Chemical Science*, 4(1) (2016) 40–49.

[10] Bal S., Orhan B., Connolly J. D., Dığrak M., Köytepe S., Synthesis and characterization of some Schiff bases, their metal complexes and thermal, antimicrobial and catalytic features, *J. Therm. Anal. Calorim.*, 121 (2015) 909–917.

[11] Erdem O., Guzel B., Synthesis, characterization and catalytic activity of chiral binaphthyl Schiff-base manganese complexes for the epoxidation of styrene, *Inorganica Chimica Acta*, 418 (2014) 153-156.

[12] Bal S., Connolly J. D., Synthesis, characterization, thermal and catalytic properties of a novel carbazole derived Azo ligand and its metal complexes, *Arabian Journal of Chemistry*, 10 (2017) 761–768.

[13] Amirnasr M., Bagheri M., Farrokhpour H., Schenk K. J., Mereiter K., Ford P. C., New Zn(II) complexes with N2S2 Schiff base ligands. Experimental and theoretical studies of the role of Zn(II) in disulfide thiolate-exchange, *Polyhedron*, 71 (2014) 1-7.

[14] Çakmak R., Ay B., Çınar E., Başaran E., Akkoç S., Boğa M., Taş E., Synthesis, spectroscopic, thermal analysis and in vitro cytotoxicity, anticholinesterase and antioxidant activities of new Co(II), Ni(II), Cu(II), Zn(II), and Ru(III) complexes of pyrazolone-based Schiff base ligand, *Journal of Molecular Structure*, 1292 (2023) 136225.

[15] Al Zoubi W., Al-Hamdani A. A. S., Ko Y. G., Schiff bases and their complexes: Recent progress in thermal analysis, *Separation Science and Technology*, 52(6) (2017) 1052-1069.

[16] de Toledo T. A., da Costa R. C., da Silva L. E., Teixeria A. M. R., Lima V. N., Sena Jr D. M., Coutinho H. D. M., Freire P. T. C., Pizani P. S., Thermal and biological properties of the Schiff base N,N′-bis(salicylidene)-1,2-phenylenediamine, a potential adjuvant to antibiotic therapy, *Journal of Molecular Structure*, 1115 (2016) 105-108.

[17] Ozkinali S., Yavuz S., Tosun T., Kose D. A., Gur M., Kocaokutgen H., Synthesis, Spectroscopic and Thermal Analysis and Investigation of Dyeing Properties of o-Hydroxy Schiff Bases and Their Metal Complexes, *Journal of Molecular Structure*, 40(5) (2020) 12624-12634.

[18] Hu Q., Li H., Wang L., Gu H., Fan C., DNA Nanotechnology-Enabled Drug Delivery Systems, *Chem. Rev.*, 119 (2019) 6459–6506.

[19] Pages B. J., Ang D. L., Wright E. P., Aldrich-Wright J. R., Metal complex interactions with DNA, *Dalt. Trans.*, 44 (2015) 3505–3526.

[20] Damercheli M., Dayyani D., Behzad M., Mehravi B., Shafiee Ardestani M., New salen-type manganese(III) Schiff base complexes derived from meso - 1,2-diphenyl-1,2-ethylenediamine: in vitro anticancer activity, mechanism of action, and molecular docking studies, *J. Coord. Chem.*, 68 (2015) 1500–1513.

[21] da Silveira V. C., Luz J. S., Oliveira C. C., Graziani I., Ciriolo M. R., da C. Ferreira A. M., Double-strand DNA cleavage induced by oxindole-Schiff base copper(II) complexes with potential antitumor activity, *J. Inorg. Biochem.*, 102 (2008) 1090–1103.

[22] Zeng Y. B., Yang N., Liu W. S., Tang N., Synthesis, characterization and DNA-binding properties of La(III) complex of chrysin, *J. Inorg. Biochem.*, 97 (2003) 258–264.

[23] Kose A., Gungor O., Ballı J. N., Erkan S., Synthesis, characterization, non-linear optical and DNA binding properties of Schiff base ligand and its Cu(II) and Zn (II) complexes, *Journal of Molecular Structure*, 1268 (2022) 133750.

[24] Bal M., Kose A., Schiff bases containing 1,2,3-triazole group and phenanthroline: Synthesis, characterization, and investigation of DNA binding properties, *Journal of Photochemistry & Photobiology, A: Chemistry*, 448 (2024) 115320.

[25] Turgut E., Gungor O., Kirpik H., Kose A., Gungor S. A., Kose M., Benzimidazole ligands with allyl, propargyl or allene groups, DNA binding properties, and molecular docking studies, *Applied Organometallic Chemistry*, 35 (2021) e6323.

[26] Gungor O., Kocer F., Kose M., Cu(II) complexes of biguanidine ligands: Structural characterisation, DNA binding and antimicrobial properties, *Journal of Molecular Structure*, 1204 (2020) 127533.

[27] Finnie K. S., Bartlett J. R., Woolfrey J. L., Vibrational Spectroscopic Study of the Coordination of (2,2‘-Bipyridyl-4,4‘-dicarboxylic acid)ruthenium(II) Complexes to the Surface of Nanocrystalline Titania, *Langmuir*, 14(10) (1998) 2744-2749.

[28] Deacon G. B., Phillips R. J., Relationships between the carbon-oxygen stretching frequencies of carboxylato complexes and the type of carboxylate coordination, *Coordination Chemistry Reviews*, 33(3) (1980) 227-250.

[29] Tiwari M. K., Singh A. K., Sawhney K. J. S., Analysis of stainless steel samples by energy dispersive X-ray fluorescence (EDXRF) spectrometry, *Bulletin of Materials Science*, 24(6) (2001) 633-638.

[30] Roy G. B., Synthesis and study of physico-chemical properties of a new chiral Schiff base ligand and its metal complex, *Inorganica Chimica Acta*, 362(6) (2009) 1709-1714.

[31] El-Seidy A. M. A., In Situ Room Temperature Synthesis and Characterization of Salicylaldehyde Phenylhydrazone Metal Complexes, Their Cytotoxic Activity on MCF-7 Cell Line, and Their Investigation as Antibacterial and

Antifungal Agents, *Inorganic and Nano-Metal Chemistry*, 45(3) (2015) 437-446.

[32] Shennar K. A., Butcher R. J., Greenaway F. T., Co(II), Cu(II), Mn(II) and Ni(II) complexes of maleic hydrazide, *Inorganica Chimica Acta*, 425 (2015) 247-254.

[33] El-Sayed A. E. M., Al-Fulaij O. A., Elaasar A. A., El-Defrawy M. M., El-Asmy A. A., Spectroscopic characterization and biological activity of dihydrazone transition metal complexes: Crystal structure of 2, 3-butanedione bis (isonicotinylhydrazone), *Spectrochimica Acta Part A: Molecular and Biomolecular Spectroscopy*, 135 (2015) 211-218.

[34] Wolfe A., Shimer Jr G. H., Meehan T., Polycyclic aromatic hydrocarbons physically intercalate into duplex regions of denatured DNA, *Biochemistry*, 26(20) (1987) 6392-6396.

[35] Reinhardt C. G., Krugh T. R., A comparative study of ethidium bromide complexes with dinucleotides and DNA: direct evidence for intercalation and nucleic acid sequence preferences, *Biochemistry*, 17(23) (1978) 4845-4854.

[36] Rajesh J., Rajasekaran M., Rajagopal G., Athappan P., Analytical methods to determine the comparative DNA binding studies of curcumin–Cu (II) complexes, *Spectrochimica Acta Part A: Molecular and Biomolecular Spectroscopy*, 97 (2012) 223-230.

[37] Kumar N., Kaushal R., Awasthi P., Non-covalent binding studies of transition metal complexes with DNA: A review, *Journal of Molecular Structure*, 1288 (2023) 135751.

[38] Ali M. S., Muthukumaran J., Al-Lohedan H. A., Molecular interactions of ceftazidime with bovine serum albumin: Spectroscopic, molecular docking, and DFT analyses, *Journal of Molecular Liquids*, 313 (2020) 113490.

[39] Abdel-Rahman L. H., Abu-Dief A. M., Abdel-Mawgoud A. A. H., Development, structural investigation, DNA binding, antimicrobial screening and anticancer activities of two novel quari-dentate VO (II) and Mn (II) mononuclear complexes, *Journal of King Saud University-Science*, 31(1) (2019) 52-60.

[40] Afrin M., Gaurav A. K., Yang X., Pan X., Zhao Y., Li B., Tb RAP1 has an unusual duplex DNA binding activity required for its telomere localization and VSG silencing, *Science Advances*, 6(38) (2020) eabc4065.

[41] Gehlen M. H., The centenary of the Stern-Volmer equation of fluorescence quenching: From the single line plot to the SV quenching map, *Journal of Photochemistry and Photobiology C: Photochemistry Reviews*, 42 (2020) 100338.

[42] Luck G., Zimmer C., Conformational aspects and reactivity of DNA. Effects of manganese and magnesium ions on interaction with DNA, *European Journal of Biochemistry*, 29(3) (1972) 528-536.

[43] Siddiqui S., Ahmed N., Goswami M., Chakrabarty A., Chowdhury G., DNA damage by Withanone as a potential cause of liver toxicity observed for herbal products of Withania somnifera (Ashwagandha), *Current Research in Toxicology*, 2 (2021) 72-81.

[44] Yoon K. R., Ko S-O., Lee S. M., Lee H., Synthesis and characterization of carbazole derived nonlinear optical dyes, *Dyes and Pigments*, 75 (2007) 567-573.

[45] Grigoras M., Antonoaia N. C., Synthesis and characterization of some carbazolebased imine polymers, *European Polymer Journal*, 41 (2005) 1079-1089.